Published in final edited form as:
Mol Cell Neurosci. 2010 October ; 45(2): 180–191. doi:10.1016/j.mcn.2010.06.009.

Layer I as a putative neurogenic niche in young adult guinea pig cerebrum

Kun Xiong[1,#], **Yan Cai**[1,2,3,#], **Xue-Mei Zhang**[3,4,#], **Ju-Fang Huang**[1], **Zhong-Yu Liu**[5], **Guang-Ming Fu**[5], **Jia-Chun Feng**[4], **Richard W. Clough**[2], **Peter R. Patrylo**[2,3], **Xue-Gang Luo**[1], **Chun-Hong Hu**[5], and **Xiao-Xin Yan**[2,*]

[1]Department of Anatomy and Neurobiology, Central South University Xiangya Medical School, Changsha, Hunan 410013, China

[2]Department of Anatomy, Southern Illinois University School of Medicine, Carbondale, IL 62901, USA

[3]Department of Physiology, Southern Illinois University School of Medicine, Carbondale, IL 62901, USA

[4]Department of Neurology, The First Hospital of Jilin University, Changchun, Jilin 130021, China

[5]Department of Oncology, Second Xiangya Hospital, Central South University, Changsha, Hunan 410011, China

Abstract

A considerable number of cells expressing typical immature neuronal markers including doublecortin (DCX+) are present around layer II in the cerebral cortex of young and adult guinea pigs and other larger mammals, and their origin and biological implication await further characterization. We show here in young adult guinea pigs that these DCX+ cells are accompanied by in situ cell division around the superficial cortical layers mostly in layer I, but they co-express proliferating cell nuclear antigen and an early neuronal-fate determining factor, PAX6. A small number of these DCX+ cells also colocalize with BrdU following administration of this mitotic indicator. Cranial X-ray irradiation causes a decline of DCX+ cells around layer II, and novel environmental exploration induces c-Fos expression among these cells in several neocortical areas. Together, these data are compatible with a notion that DCX+ cortical neurons around layer II might derive from proliferable neuronal precursors around layer I in young adult guinea pig cerebrum, and that these cells might be modulated by experience under physiological conditions.

Keywords

marginal zone; adult neurogenesis; neuroplasticity; corticogenesis; brain evolution

Introduction

During the past few decades, the development of new cell birth-dating technologies and identification of endogenous cell proliferation and early neuronal differentiation markers have led to a revolutionary understanding of neurogenesis in the adult mammalian brain (Gross, 2000; Gould, 2007; Zhao et al., 2008). To date, it is generally accepted that the

*Correspondence to: Xiao-Xin Yan, Department of Anatomy, Southern Illinois University at Carbondale, 1135 Lincoln Drive, #2069 Life Science III, Carbondale, IL 62901-6525; Tel: 618-453-6536; Fax: 618-453-6527; xyan@siumed.edu.
#Authors contributed equally to this work

subventricular and subgranular zones (SVZ, SGZ) produce new neurons, which may be important for olfaction and hippocampus-related cognitive functions (Bruel-Jungerman et al., 2007; Deng et al., 2010). As with the adult-born SVZ and SGZ neuronal population, many cells located around cortical layer II express typical immature neuronal markers including doublecortin (DCX+), more prominent in larger mammals relative to small laboratory rodents (Seki and Arai, 1991; Bonfanti et al., 1992; Nacher et al., 2001; Xiong et al., 2008; Liu et al., 2008; Luzzati et al., 2009; Cai et al., 2009; Srikandarajah et al., 2009). Recent data indicate that these DCX+ cells are immature and developing neurons undergoing differentiation and maturation into putative GABAergic subgroups (Shapiro et al., 2007; Gómez-Climent et al., 2008; Cai et al., 2009). Controversy exists in regard to whether these cells are generated prenatally (Gómez-Climent et al., 2008; Luzzati et al., 2009) or possibly during postnatal and adult life (Bernier et al.,2002; Tonchev et al.,2003; Pekcec et al.,2006; Shapiro et al., 2007). Also, while some authors propose that these cells may derive from the SVZ (Bernier et al.,2002; Tonchev et al.,2003; Pekcec et al., 2006; Shapiro et al., 2009), it is also speculated that they might actually arise from local or nearby neurogenic sites (Xiong et al.,2008; Cai et al., 2009).

The SVZ and several subpallial structures are the major sites to generate cortical principal neurons and interneurons (Berry and Rogers, 1965; Rakic, 1972; Anderson et al., 1997; Lavdas et al., 1999; Wichterle et al., 2001; Letinic et al., 2002). However, in rodents as well as primates the marginal zone and its derivative layer I exhibit mitotic activity (Raedler and Raedler, 1978; Marin-Padilla, 1978; Choi, 1988; Meyer et al., 1998; Bystron et al., 2006). Recent studies demonstrate that in rat and mouse the marginal zone/layer I produce interneurons in postnatal/adult life (Costa et al., 2007; Ohira et al., 2010). Also of note is that the marginal zone/layer I may become more complicated structurally with mammalian evolution (Meyer et al., 1998; Zecevic and Rakic, 2001; Rakic and Zecevic, 2003). We hypothesize that DCX+ immature neurons around layer II, an interface region between the original marginal zone and cortical plate, might derive from neurogenesis in layer I and be modulated by behavioral stimuli or cortical network activity under physiological conditions in young adult guinea pigs. The present study investigated these possibilities using an combined approach by examining: (1) the expression of proliferative and early neuronal fate-determining markers relative to DCX around layers I and II; (2) the possibility of 5-bromo-2′-deoxy-uridine (BrdU) incorporation into these cortical DCX+ cells; (3) effect of cranial X-ray irradiation on these cells; and (4) c-Fos induction in these cells following novel environmental exploration.

Results

In situ cell proliferation around cortical layers I/II

Cells expressing Ki67 (Ki67+), pH3 (pH+) and PCNA (PCNA+) were consistently detectable in layers I and II across the cortical hemisphere in 3-7 month-old guinea pigs examined in the present study, with a few labeled cells also seen in deeper cortical layers (Supplementary Fig. 2A-F). Labeled cells in layer I occurred across this layer including at the pia mater. All labeled profiles were nuclei as confirmed by hematoxylin or bisbenzimide counterstain, with some appeared in pairs or in small clusters (inserts in Supplementary Fig. 2A-F; Fig. 1A1, E2, F-H).

At 3 hours after a single BrdU injection (50 mg/kg, i.p.), BrdU+ cells were detected across cortical layers I-VI, again mostly in layers I and II (Supplementary Fig. 2G-J). At the 72 hours surviving point, many BrdU+ cells occurred in pairs (Supplementary Fig. 2K-M). We carried out preliminary laminar distribution analyses of BrdU+ cells over representative cortical regions (in neutral red counterstained sections), including the parietal (3 levels passing the striatum, 180 μm apart) and temporal (3 levels passing the amygdale, 360 μm

apart) neocortices. Among all BrdU+ cells over layers I-VI, more than two-thirds of the cells were located in layers I/II at 3 and 72 hours in both cortical regions. For example, in the temporal neocortex, 71.8 ± 7.9% (mean ± SD, among 2642 counted cells from 3 animals) and 67.4 ± 9.1% (among 4177 cells) BrdU+ cells resided in layers I and II at 3 and 72 hours post-BrdU injection, respectively.

Colocalization of mitotic and neuronal fate-determining markers among cortical DCX+ cells

Across the cerebral hemisphere, Ki67 and pH3 labelings in layers I and II were virtually always colocalized (data not shown). While neither marker colocalized in DCX+ cells, DCX + and Ki67+/pH3+ cells might occur next to each other around layer II (Fig. 1A, B). PCNA labeling was found to partially colocalize in many small DCX+ cells around the border of layers I and II (Fig. 1C-E). To understand the above differential DCX colocalization with the endogenous mitotic markers, we performed double labelings for Ki67 and pH3 (data not shown) with PCNA. Brightly stained PCNA+ nuclei in layers I and II co-expressed Ki67 (Fig. 1F-I) or pH3, which had relatively large size and often occurred in pairs, optimal for S-M phase morphochemical configurations. In contrast, small and weakly stained PCNA+ nuclei did not colocalize with Ki67 or pH3 (Fig. 1F′-I′), which might be at other cell cycle phases or at early postmitotic state. Thus, PCNA expression appeared to overlap with Ki67/pH3 expression in mitotic layer I cells during S-M phase, but extend into early stages of neuronal differentiation until after DCX onset (Fig. 1J).

The Paired Box Protein Pax-6 (PAX6) is involved in early neuronal fate determination (Zhao et al., 2008). PAX6 expression was detectable in most DCX+ cells around layer II, particularly prominent among the small-sized ones (Fig. 2A-D). Also, PAX6 reactivity colocalized with most weakly-stained PCNA+ nuclei (Fig. 2E-I), but was absent in the heavily stained PCNA+ nuclei (Fig. 2I). No PAX6 labeling was found in Ki67+ or pH3+ cells (not shown). Therefore, PAX6 expression appeared to overlap partially with both PCNA and DCX expression, but emerge after Ki67/pH3 expression among layers I/II cells (Fig. 2J).

GFAP is expressed in neuroblasts around the SVZ and SGZ (Ihrie and Alvarez-Buylla, 2008; Zhao et al., 2008). GFAP+ astrocytes-like cells occurred along the pia mater, some of which co-expressed PCNA (Fig. 2K-L, yellow arrows). However, subpial PCNA+ cells (in layers I and II) did not colocalize with GFAP (Fig. 2K-L, white arrows). Around the lateral ventricle, GFAP and PCNA colocalized commonly among the ependymal layer cells (Fig. 2N, O). Some PCNA+ cells in the subventricular zone also co-expressed GFAP (Fig. 2P, P′). Therefore, putative proliferating GFAP+ cells existed similarly around the pial and ventricular surfaces (Fig. 2M, Q).

Colocalization of BrdU in DCX+ cortical cells in BrdU pulse-chase analysis

Double immunofluorescence was performed on 6 μm-thick sections to assess BrdU colocalization with DCX and NeuN, respectively, at various surviving time points (7-90 days) after 4 consecutive BrdU injections (Supplementary Fig. 1). Double-labeled profiles were confirmed by a precise colocalization of BrdU with bisbenzimide nuclear labeling, with some also verified with a FluoView™ FV1000 Olympus confocal microscope using z-stack scanning (Fig. 3A-E). Overall, BrdU+ nuclei were found in layers I and II at all surviving time points, mostly small, and many appeared in pairs or small cluster even at the long surviving time points (60 and 90 days).

Only a small number of BrdU/DCX double-labeled cells were detected around layer II at each surviving time among a substantial number of counted BrdU+ cells (Fig. 3). Thus,

BrdU+/DCX+ cells were 1.7 ± 1.4% (mean ± S.D., 20/1279) at 7 days, 1.8 ± 0.8 % (24/1362) at 14 days, 2.4 ± 0.4 % (31/1325) at 30 days, 0.8 ± 0.6 % (9/1151) at 60 days, and 0.2 ± 0.4 % (3/1307) at 90 days post-BrdU administration (Fig. 3I). All double-labeled cells were small, lacked apparent dendritic or axonal processes and often occurred in clusters (Fig. 3A-E). It should be noted that singly labeled BrdU+ nuclei might tightly appose to singly labeled DCX+ cells, and they appeared to form a same cell cluster (Fig. 3F, G). In some cases, BrdU+ nuclei appeared to be shrinking or deformed (Fig. 3H). Despite thorough search in multiple sections from each brain, we were unable to find clear BrdU colocalization with NeuN+ neurons in the cortex in the present study.

Colocalization of mitotic and immature neuronal markers in the SVZ/SGZ

We cross-validated the authentic labelings of proliferative and immature neuronal markers in the guinea pig brains by using the SVZ and SGZ as internal references, and similar colocalization patterns were found between these two sites. Thus, PCNA labeling partially colocalized with DCX+ cells at the SVZ (Fig. 4A-C), similar to the pattern seen around layer II. Also as with layers I/II, Ki67 reactivity occurred in the nuclei of SVZ/SGZ cells with strong PCNA labeling, but not in those with weak PCNA labeling (Fig. 4D-F). In contrast to layer II, Ki67 labeling occurred in some DCX+ cells at the SVZ (not shown) and SGZ (Fig. 4G-I). At 3 hours after a single BrdU injection, BrdU labeling colocalized partially with Ki67 (Fig. 4J-M) and PCNA (Fig. 4N-P) in the SVZ/SGZ. PCNA+/BrdU+ nuclei appeared to express brighter PCNA labeling relative to PCNA+/BrdU- cells (Fig. 4N-P). From 7 days onward, BrdU+/DCX+ cells occurred clearly in the SVZ or SGZ, and importantly, the double-labeled neurons had well-developed dendritic processes (Fig. 4Q-R).

Decline of DCX+ and Ki67+ cells in layers I/II, SVZ and SGZ after X-ray irradiation

A unilateral X-ray irradiation paradigm was used to determine whether this treatment might lead to reduction of DCX+ and Ki67+ cells around layers I/II and the SVZ/SGZ in the ipsilateral hemisphere relative to its internal control, the contralateral side (Wojtowicz, 2006). Pilot studies used single dosage radiations at 10 and 15 Gy, and brains were examined at 7 and 30 days post-radiation (n=3/dose/time point). There were dramatic decline of DCX+ and Ki67+ cells in the SVZ/SGZ and also visually noticeable decline of Ki67+ cells in layers I and II at both time points. However, the amount of DCX labeling around layer II appeared comparable microscopically between the two sides, and preliminary cell count analysis did not yield significant difference in these cells between the radiated and control sides (data not shown). In subsequent formal experiments, 3 month-old guinea pigs received 3 times of X-ray irradiation, each at 5 Gy, on day 1, 7 and 14 (Supplementary Figs. 1, 3, 4; Figs. 5, 6).

Compared to the control side, DCX+ cells in layer II were reduced in the radiated side across the anterioposterior dimension of cerebrum at 21 days post-radiation (Fig. 5B-F). Densitometric analyses over 3 representative cortical regions indicated a parallel decline of DCX+ cells in the radiated relative to the control sides among these analyzed regions (Fig. 6A, B). Thus, the densities of DCX+ cells (# of cells/mm pial length) were 83.1 ± 13.1 (mean ± SD, same format below) and 122.8 ± 19.4 in the radiated and control sides, respectively, of the parietal neocortex, with statistically significant difference between the two sides ($p<0.05$, one-way ANOVA, by Bonferroni's multiple mean comparison tests, same below). Similarly, the densities of DCX+ cells were reduced in the radiated (98.4 ± 21.7) relative to the control (143.2 ± 30.6) temporal lobe cortex (TLC, including the neocortical and entorhinal areas) ($p<0.01$), as well as in the radiated (187.2 ± 27.4) relative to control (282.2 ± 46.7) piriform cortex ($p<0.001$). As expected, DCX+ cells around the SVZ were greatly reduced in the radiated (7.2 ± 2.7) relative to control (78.8 ± 25.7) ($p<0.001$) sides.

Further, DCX+ cells in the radiated dentate SGZ (19.4 ± 6.5) were dramatically reduced relative to counterpart (257.7 ± 26.1) ($p<0.001$). The extent of decline in DCX+ cells in the radiated forebrain areas (normalized to corresponding controls) was comparable among the parietal (67.7 ± 10.7%), temporal lobe (68.7 ± 15.1%) and piriform (65.8 ± 9.6%) cortices, and between the SVZ (9.2 ± 3.4%) and the SGZ (7.6 ± 2.6%), but was significantly greater in the SVZ and the SGZ relative to the cortical regions ($p<0.0001$, one-way ANOVA, F=34.7, df=4, 10).

Ki67+ cells were dramatically reduced around layers I/II, the SVZ and the SGZ in the radiated relative to the control sides at 21 post-radiation (Supplementary Fig. 3). Because the extents of change in Ki67+ cells were comparable among the cortical regions, we included the densitometric data from the TLC, SVZ and SGZ (Fig. 6A). Thus, the densities of Ki76+ cells in layers I and II of the TLC were lower in the radiated (0.95 ± 0.05, mean ± SD, # of cells/mm pial length) relative to the control (9.7 ± 2.3) sides ($p<0.05$, one-way ANOVA, by Bonferroni's multiple mean comparison tests). Similarly, Ki67+ cells in the SVZ were significantly reduced in the radiated side (13.6 ± 2.7, # of cells/mm ventricular surface length) compared to control (99.6 ± 3.4) ($p<0.001$). Moreover, Ki67+ cells in the SGZ declined significantly in the radiated dentate gyrus (2.2 ± 0.53, # of cells/mm length of the GCL) relative to internal control (23.6 ± 2.6) ($p<0.001$) (Fig. 6C).

We examined DCX+ and Ki67+ cells in the forebrain at 3 later surviving time points (56, 90 and 120 days) to assess whether these cells might show trend of recovery (Fig. 6D-F; Supplementary Fig. 3). To avoid redundancy (i.e., among cortical regions and between the SVZ and SGZ), we included here densitometric data of DCX+ cells in the TLC and dentate gyrus (Fig. 6D, E), and relative densities of these cells in the radiated side normalized to the control side at each surviving point (Fig. 6F). Thus, DCX+ cells in the radiated TCL showed trend of recovery after 56 days post-radiation, although remained lower relative to controls even at 120 days (Fig. 6D). The densities of DCX+ cells in the dentate gyrus remained less in the radiated side at 56 and 90 days, but approached control levels by 120 days (Fig. 6E). In sum, relative densities of DCX+ cells in the radiated TLC were 68.7 ± 15.1%, 57.1 ± 13.2%, 51.7 ± 12.0% and 70.7 ± 19.9% of the control side at 21, 56, 90 and 120 days, respectively. Ki67+ cell densities in the radiated TLC were 10.8 ± 3.8%, 49.7 ± 12.5%, 96.2 ± 10.6% and 91.1 ± 15.0% of non-radiated side at these time points. The densities of DCX+ cells in the dentate gyrus were 9.6 ± 3.2%, 23.1 ± 10.9%, 54.5 ± 10.7% and 82.0± 14.6% of the control levels at 21, 56, 90 and 120 days. The densities of Ki67+ cells in the dentate gyrus were 9.2 ± 3.2%, 84.3 ± 10.3%, 98.3 ± 8.7% and 97.6± 9.9% of controls at the above time points. Thus, cell type-wise, Ki67+ cells in the radiated cortex and dente gyrus tended to recover earlier relative to DCX+ cells. Regionally, the recovery of DCX+ and Ki67+ cells appeared to occur earlier in the dentate gyrus relative to the cortex.

c-Fos induction in DCX+ cortical neurons following novel environmental exploration

Stimulation/experience induced c-Fos expression may reflect whether a particular group of neurons may be integrated into functional neural networks under physiological conditions (Tashiro et al., 2007; Ohira et al., 2009). We explored c-Fos induction in DCX+ cells over representative neocortical areas, including the medial prefrontal (mPFC), primary somatosensory (SM1) and primary visual (V1) cortices using a novel environmental exploration paradigm. The environmental exposure study was carried out in the early morning (7AM) to minimize environmental disturbances. Experimental animals were first exposed to an enriched arena for 30 minutes (Fig. 7A), then returned to and stayed in their home cages for 60 minutes to allow c-Fos induction. Controls animals were maintained in the home cages during this same period.

In the control animals, only a small number of DCX+ cortical cells co-expressed c-Fos, and they had relatively large somata and well-developed dendrites (Fig. 7B-F). In contrast, many DCX+ cortical cells, small and large ones alike, colocalized with c-Fos in the experimental animals (Fig. 7B, G-J). Quantitatively, 31.7 ± 10.3% (mean ± SD) DCX+ cells in the mPFC co-expressed c-Fos (737 among a total of 2229 counted cells from 3 animals) in the experimental group, whereas only 3.1 ± 1.0% DCX+ cells (77/2508) colocalized with c-Fos in the control group ($p<0.05$, n=3, two-tail paired students-*t* test). In the SM1, 17.9 ± 2.4% (479/2790) and 4.8 ± 1.8% (89/1905) double-labeled cells were recorded in the experimental and control groups, respectively, with statistically significant difference between the two groups ($p<0.01$, n=3, two-tail paired students-*t* test). Moreover, DCX+ cells co-expressing c-Fos were increased in the V1 in the experimental (12.9 ± 1.2%, 301/2327) relative to control groups (4.1 ± 1.3%, 88/2050) ($p<0.05$, n=3, two-tail paired students-*t* test) (Fig. 7B).

Discussion

DCX+ cortical cells may derive from layer I neurogenesis in young adult guinea pigs

Using the BrdU birth-dating method, previous studies have attempted to determine where and when the DCX+ or PSA-NCAM+ cells present in cortical layer II of young or adult mammals might be generated. The SVZ is proposed as the origin of these cells among reports, although the laminar distribution and migratory pattern of the cells do not appear to fit well with such a notion (Cai et al., 2009). Several groups show a small rate of BrdU colocalization in piriform/temporal cortical DCX+ cells or alike in adult rodents (Pekcec et al., 2006; Shapiro et al., 2007, 2009) and nonhuman primates (Bernier et al., 2002; Tonchev et al., 2003). Shapiro and colleagues (2009) propose that the small rate of BrdU incorporation is suggestive of a slow cell cycle of the proliferating neuronal precursors that give rise to the DCX+ cortical cells in postnatal/adult brain. Other groups report no BrdU incorporation into these cortical DCX+ cells in postnatal or adult rodents (Gómez-Climent et al., 2008) and rabbits (Luzzati et al., 2009). Gómez-Climent et al (2008) also show that all PSA-NACM+ cells in 3 month-old rat piriform cortex colocalize with BrdU after administration of this mitotic marker at embryonic (E) day E11.5 (2%), E13.5 (23.5%) and E15.5 (74.7%). The authors conclude that these piriform cortical immature neurons are generated prenatally during the same period as with the nearby pyramidal neurons (Fig. 2K in Gómez-Climent et al., 2008). However, it is somewhat puzzling that the collective rate of BrdU/PSA-NCAM colocalization from the 3 above time points is already “fully saturated” (totaled 100.2%), giving that the bioavailability of BrdU to be incorporated into DNA after an i.p. injection is perhaps only a few hours (Kriss et al., 1963; Packard et al., 1973; Taupin, 2007). To our understanding, this saturated rate would exclude (mathematically) a possibility for any additional cells being generated at other time points between (e.g., E12.5 or E14.5) or slightly after (e.g., E16.5) the 3 examined points. Yet, the data show that the cells are generated at least during E11.5 to E15.5. Therefore, there exists a possibility of subsequent division or cycling of the proliferative cells, perhaps involving reuptake of BrdU released/“leaked” from local pyramidal cells that have incorporated this reagent (Breunig et al., 2007).

The present study uses a combined approach to explore whether and where DCX+ cells around layer II may be generated in young adult guinea pig cortex. Using endogenous mitotic markers as well as BrdU, we observe a pool of proliferating cells in layer I and neighboring II across the cerebral cortex in accompany with the DCX+ cells around layer II. Double immunofluorescence shows partial colocalization of Ki67 or pH3 with PCNA, and co-expression of PCNA and PAX6 in small and morphologically primitive DCX+ cells. These findings, according to established knowledge regarding the above markers (von Bohlen Und Halbach, 2007; Zhao et al., 2008), would be most simply explained as to depict a cellular trajectory that begins with mitosis (Ki67/pH3/PCNA+) and subsequent neuronal

fate commitment (PCNA+ → PAX6+) occurring mainly around layer I, proceeds to neuronal differentiation (DCX+) around layer II (Figs. 1J; 2J), and continues with neuronal maturation (DCX+ → NeuN+) in layer II and deeper layers (Xiong et al., 2008; Cai et al., 2009). We also find BrdU and DCX colocalization in layer II at various surviving times post-BrdU pulse administration, implicating that at least a few BrdU-incorporated local cells have become immature neurons. Moreover, X-ray irradiation attenuates Ki67 and DCX expression around layers I and II, as with the SVZ and SGZ. It should be noted that both cell proliferation and DCX expression appear to be recoverable despite of a few times of radiation. Collectively, these findings are consistent with an inhibitory effect of radiation on cell proliferation and neurogenesis (Wojtowicz, 2007), the best known cellular effect of X-ray irradiation at therapeutic dosage.

Our findings are congruent with those in late studies indicating layer I as a putative postnatal perhaps adult neurogenic niche for cortical GABAergic interneurons. For instances, PCNA colocalization in layer II DCX+ cells is recently reported in adult human temporal neocortex (Liu et al., 2008). Although DCX+ cells are rare in mouse and rat neocortex, neocortical layer I progenitors might produce some interneurons under physiological conditions in these animals (Costa et al., 2007). In fact, two most recent studies demonstrate that this superficial cortical neurogenic system may be activated by focal laser-lesion and ischemia in these animals (Sirko et al., 2009; Ohira et al., 2010).

The precise linage(s) and evolution of putative layer I neurogenic cells in guinea pigs are yet to be defined. In mice and rats, it appears that new interneurons might come from proliferable meningeal cells (Sirko et al., 2009), and neuroblasts intrinsic to layer I (Costa et al., 2007) or those derived originally from subpallial structures (Ohira et al., 2010). We observe GFAP+/PCNA+ cells at the pia mater in guinea pig cortex, which might evolve into proliferating cells located deeper (i.e., subpial layer I or layer II) (Ihrie and Alvarez-Buylla, 2008). However, PCNA+ cells at the later locations do not co-express GFAP, implicating that they might not necessarily derive from the pia-associated astrocyte-like cells, but represent intrinsic layer I neuroblasts (Fig. 2M).

Putative layer I neural progenitors exhibit novel proliferative properties

The present study reveals novel differences regarding the expression of proliferative markers and cell response to radiation between layers I/II and the SVZ/SGZ, which may be of biological implications regarding the mode/dynamics of neurogenesis/development. Unlike the SVZ and SGZ, Ki67, pH3 or GFAP colocalization with DCX is not detectable around layers I/II. These findings appear to implicate that the onset of DCX expression in putative layer I progenitors may occur later or slower relative to the SVZ/SGZ counterparts (e.g., after the cells descend to layer II).

Following a single radiation (10-15 Gy), decline of DCX+ cells was readily evident in the SVZ/SGZ but not in layer II (pilot study data). However, by splitting the same radiation dosage into 3 episodes, post-radiation decline of DCX+ cells becomes detectable around layer II, although to a lesser extent relative to the SVZ/SGZ. The findings are consistent with the fact that mitotic activity (e.g., amount of Ki67 labeling) is less abundant around layer I/II relative to the SVZ/SGZ (Supplementary Fig. 4B, D, F, H). Notably, cluster and chain organizations of DCX+ cells are fairly common around layer II (Xiong et al., 2008; Cai et al., 2009, Zhang et al., 2009), which could be a result of multiple or consecutive cell divisions. If this is the case, then it is not surprising why multiple radiations are required to cause a significant decline of DCX+ cells around layer II.

Similar to some previous reports in other species (Bernier et al., 2002; Tonchev et al., 2003; Pekcec et al., 2006; Shapiro et al., 2007), only a small rate of BrdU/DCX colocalization is

detectable around layer II in guinea pig cortex. It should be noted that many factors, including multiple cell division (causing BrdU dilution) and slow cell cycle dynamics (causing insufficient BrdU uptake), may lower the chance of successfully detecting BrdU colocalization in immature or mature neurons in BrdU pulse-chase analysis (Eisch and Mandyam, 2007; Taupin, 2007). In addition, we noticed that BrdU+ cells in layers I/II appear to mostly remain undifferentiated, which suggests cell proliferation without fate-commitment/differentiation (Breunig et al., 2007) (this however could be a result of BrdU incorporation/toxicity). We also noticed that singly-labeled BrdU+ and DCX+ cells may align as sister-like cells as if they were from the same precursor, and that some BrdU+ cells appear to be shrinking or deformed. Further, BrdU+/DCX+ double-labeled cells around layer II are small in size and have very few processes even at long surviving time points, in contrast to their counterparts around the SVZ/SGZ in the same brain that develop healthy-looking neuronal morphology. These observations point to a possibility that layer I proliferating cells might be more sensitive to BrdU toxicity relative to those in the SVZ/SGZ. In other words, the cells incorporated BrdU may commonly fail to differentiate, or perhaps dye out, causing a low or rare incidence of BrdU colocalization with DCX or NeuN around the superficial cortical layers.

Neural network activity influences DCX+ immature cortical neurons

Recent studies indicate that formation of new neurons serves a form of brain structural plasticity important for olfaction and hippocampus-dependent cognitive functions (Bruel-Jungerman et al., 2007). Meanwhile, experience and activity modulate the development and integration of newborn neurons into functional circuitries (Tashiro et al., 2007; Zhao et al., 2007; Breton-Provencher et al., 2009; Deng et al., 2010). It is therefore of interest to explore if DCX+ cortical cells may be involved in network activity under physiological conditions. Indeed, DCX+ cortical cells in young adult guinea pigs may become activated following novel environmental exploration. In home-caged controls, c-Fos expression is detectable in a few DCX+ cells with relatively large size and mature-looking morphology. Following arena exploration, c-Fos induction is detected in increasing number of DCX+ cells, both small and large ones, in the mPFC, and to a less extent, in the SM1 and V1. Therefore, DCX+ cortical cells appear to be a part of functional neural circuitry that can be modulated by sensory, motor or behavioral stimulation.

In summary, the present study provides several lines of evidence supporting a local, likely layer I, origin of novel immature neurons in the superficial cortex of young adult guinea pigs. We show similarities, yet novel differences, between putative layer I and SVZ/SGZ neuronal progenitors, especially regarding the expression/colocalization of proliferative markers and the response to radiation. Our data also suggest that these cortical immature neurons can be modulated by network activity or physiological experience. Because the brains of 3-6 months old guinea pigs are likely still undergoing development, it is possible that in fully mature guinea pigs this neurogenic potential in the cerebral cortex may be significantly reduced or even lost, as is the case for the hippocampal dentate gyrus.

Experimental Methods

Animals, BrdU administration and cranial X-ray irradiation

Male Hartley young adult guinea pigs were obtained from the animal facility of Hunan Agricultural University (Changsha, Hunan, China). Four untreated animals at 3 (n=2) and 6 (n=2) month of age were used to study the expression of endogenous proliferative and early neuronal fate-determining markers in relevance to DCX+ cortical cells. Four 3 month-old animals received one injection of 5-bromodeoxyuridine (BrdU) (B5002, Sigma-Aldrich, St Louis, MO) at 50 mg/kg (i.p.), and they were perfused 3 and 72 hours afterwards. Additional

3 month-old animals were given 4 consecutive (12 hrs apart) BrdU injections (i.p.), each at 50 mg/kg, and they were examined at 7 (n=3), 14 (n=3), 30 (n=3), 60 (n=3) and 90 (n=3) days after the last BrdU injection (Supplementary Fig. 1).

For X-ray irradiation, 3 month-old animals were anesthetized with sodium pentobarbital (50 mg/kg, i.p.). Irradiation was directed to one side of the cranium using an ELEKTA-SL18 linear medical accelerator, with 4MeV nominal photon energy and a dose rate of 200cGy/40s. A sum of 5 Gy was given at each radiation session, with 3 treatments applied to each animal at day 1, 7 and 14. Radiated animals were examined at day 21 (n=3), 56 (n=3), 90 (n=3) and 120 (n=3) (Supplementary Fig. 1). Three other animals died after two months post-radiation (20% mortality).

Animal use was in accordance with the National Institute of Health Guide for the Care and Use of Laboratory Animals. All procedures were approved by the Ethics Committee of Central South University on Animal Use.

Tissue preparation

Animals were perfused transcardially with 4% paraformaldehyde in 0.01M phosphate-buffered saline (pH 7.4, PBS) under overdose anesthesia (sodium pentobarbital, 100 mg/kg, i.p.). Brains were removed, postfixed overnight and cryoprotected in 30% sucrose. The cerebrum was cut frontally in a cryostat at 30 μm, with 12 sets of sections collected serially in PBS. Additional 6 μm sections were collected on slides by thaw-mounting for double immunofluorescence.

Immunohistochemistry

The primary antibodies used in this study included goat anti-DCX (Santa Cruz Biotech, sc-8066, diluted at 1:2000), mouse anti-neuron-specific nuclear antigen (NeuN) (Chemicon, MAB377, 1:4000), rabbit anti-Ki67 (Vector Laboratories, 014-1107, 1:1000), mouse anti-proliferating cell nuclear antigen (PCNA) (Chemicon, MAB424R, 1:10,000), rabbit anti-phosphohistone-3 (pH3) (Epitomics, 1329-1, 1:1000), rat anti-BrdU (Serotec, MCA2060, 1:2000); rabbit anti-PAX6 (Covance, PRB-278P, 1:2000), rabbit anti-glial fibrillary acidic protein (GFAP) (Sigma-Aldrich, G9269, 1:4000), rabbit anti-c-Fos (Santa Cruz Biotech, sc-52, 1:4000).

To visualize immunoreactivity with the peroxidase method, sections were treated with 3% H_2O_2 for 30 minutes, then with 10% normal horse or rabbit serum in PBS with 0.1 % Triton X-100 for 1 hour. Sections were then incubated with a primary antibody overnight in PBS with 5% blocking serum. Sections were then reacted with biotinylated horse anti-mouse, rabbit and goat IgGs, or rabbit anti-rat IgG at 1:400 for 2 hours, and subsequently with the ABC reagents (1:400) (Vector Laboratories, Burlingame, CA) for 1 hour. Immunoreation products were visualized in 0.003% H_2O_2 and 0.05% DAB together with 0.025% NiCl and 0.025% CoCl in some cases. For BrdU immunolabeling, sections were treated in 1 × SSC and 50% formamide for 1 hour at 65 °C, then in 2N HCl for 30 minutes at 37 °C, before H_2O_2 treatment. All incubations were followed by three 10-minute washes, and the sections were dehydrated and mounted.

For double immunofluorescence, sections were incubated in PBS containing 5% donkey serum, 0.1% Triton X-100 and a pair of the primary antibodies from different species overnight at 4 °C. Sections were further incubated for 2 hours at room temperature in PBS containing Alexa-Fluor® 488 and Alexa-Fluor® 594 conjugated donkey anti-mouse, rat, rabbit or goat IgGs (1:200, Invitrogen, Carlsbad, CA). Sections were finally counter-stained with bisbenzimide (Hoechst 33342, 1:50000), washed, and mounted with anti-fading medium.

In this study, omission of the primary antibodies in the incubation buffer or substitution of a given antibody with normal serum from its host animal species yielded no specific labeling. No any BrdU+ profiles were observed in sections from animals that did not receive BrdU treatment.

Imaging and densitometry

Sections were examined and imaged with an Olympus fluorescent BX60 microscope equipped with a digital imaging system (MicroFire® CCD Camera and software, Optronics, Goleta, CA). For densitometry, images over selected cortical, hippocampal and periventricular regions were captured continuously using a 10× objective along the pia mater, the ventricular wall or the granule cell layer (GCL). Labeled cells around layers I and II, the SVZ and the SGZ were then counted in each image, and totaled for each section. The length of corresponding pial surface, ventricular wall or GCL in the same image was measured and also totaled for each section. Cell densities were expressed as number of cells per millimeter length of pial surface, the ventricular wall or the GCL using the above data.

To quantify the rate of BrdU colocalization with DBX, we examined 2 sets of 6 μm sections from each brain, with each set passing ~10 rostrocaudal levels in equal intervals (~2 mm). Sections were scanned tangentially across the cortical hemispheres at 40× (covering ~300 μm depth from deep layer I to layer II). All encountered BrdU+ cells were checked for colocalization with DCX, with BrdU+ only and BrdU+/DCX+ double-labeled cells recorded. A similar method was used for quantifying c-Fos and DCX colocalization around layer II in the medial prefrontal (mPFC), primary somatosensory (SM1) and primary visual (V1) cortices. Some double-labeled profiles were re-examined using a confocal microscope (Olympus Fluoview, Japan). There was essentially no cell overlap in the 6 μm-thick sections used for double immunofluorescence.

Statistical testing and figure preparation

Means of cell densities or rate of colocalization were analyzed statistically using one-way ANOVA with Bonferroni's pair-wise multiple comparisons, or students-*t* test (Prism GraphPad 4.1, San Diego, CA). The minimal significant level of difference was set at $p < 0.05$. Figures were prepared with Photoshop 7.1, converted into TIFF files, with contrast/brightness adjusted as needed.

Supplementary Material

Refer to Web version on PubMed Central for supplementary material.

Acknowledgments

This study was supported in part by Natural Science Foundation of China (#30900773 to K.X., X.X.Y.), Illinois Department of Public Health (X.X.Y.), National Institute of Health (1R21NS056371 to P.R.P., X.X.Y), and the Center for Alzheimer's Disease and Related Disorders of Southern Illinois University School of Medicine.

References

Anderson SA, Eisenstat DD, Shi L, Rubenstein JL. Interneuron migration from basal forebrain to neocortex: dependence on Dlx genes. Science 1997;278:474–476. [PubMed: 9334308]

Berry M, Rogers AW. The migration of neuroblasts in the developing cerebral cortex. J Anat 1965;99:691–709. [PubMed: 5325778]

Bernier PJ, Bédard A, Vinet J, Lévesque M, Parent A. Newly generated neurons in the amygdale and adjoining cortex of adult primates. Proc Natl Acad Sci USA 2002;99:11464–11469. [PubMed: 12177450]

Bonfanti L, Olive S, Poulain DA, Theodosis DT. Mapping of the distribution of polysialylated neural cell adhesion molecule throughout the central nervous system of the adult rat: an immunohistochemical study. Neuroscience 1992;49:419–436. [PubMed: 1436474]

Breton-Provencher V, Lemasson M, Peralta MR 3rd, Saghatelyan A. Interneurons produced in adulthood are required for the normal functioning of the olfactory bulb network and for the execution of selected olfactory behaviors. J Neurosci 2009;29:15245–15257. [PubMed: 19955377]

Bruel-Jungerman E, Davis S, Laroche S. Brain plasticity mechanisms and memory: a party of four. Neuroscientist 2007;13:492–505. [PubMed: 17901258]

Breunig JJ, Arellano JI, Macklis JD, Rakic P. Everything that glitters isn't gold: a critical review of postnatal neural precursor analyses. Cell Stem Cell 2007;1:612–627. [PubMed: 18371403]

Bystron I, Rakic P, Molnar Z, Blakemore C. The first neurons of the human cerebral cortex. Nat Neurosci 2006;9:880–886. [PubMed: 16783367]

Cai Y, Xiong K, Chu Y, Luo DW, Luo XG, Yuan XY, Struble RG, Clough RW, Spencer DD, Williamson A, Kordower JH, Patrylo PR, Yan XX. Doublecortin expression in adult cat and primate cerebral cortex relates to immature neurons that develop into GABAergic subgroups. Exp Neurol 2009;216:342–356. [PubMed: 19166833]

Choi BH. Developmental events during the early stage of cerebral cortical neurogenesis in man. A correlative light, electron microscopic, immunohistochemical and Golgi study. Acta Neuropathol 1988;75:441–447. [PubMed: 2454011]

Costa MR, Kessaris N, Richardson WD, Götz M, Hedin-Pereira C. The marginal zone/layer I as a novel niche for neurogenesis and gliogenesis in developing cerebral cortex. J Neurosci 2007;27:11376–11388. [PubMed: 17942732]

Deng W, Aimone JB, Gage FH. New neurons and new memories: how does adult hippocampal neurogenesis affect learning and memory? Nat Rev Neurosci. 2010 Epub ahead of print.

Eisch AJ, Mandyam CD. Adult neurogenesis: can analysis of cell cycle proteins move us “Beyond BrdU”? Curr Pharm Biotechnol 2007;8:147–165. [PubMed: 17584088]

Gómez-Climent MA, Castillo-Gómez E, Varea E, Guirado R, Blasco-Ibáñez JM, Crespo C, Martínez-Guijarro FJ, Nácher J. A population of prenatally generated cells in the rat paleocortex maintains an immature neuronal phenotype into adulthood. Cereb Cortex 2008;18:2229–2240. [PubMed: 18245040]

Gould E. How widespread is adult neurogenesis in mammals? Nat Rev Neurosci 2007;8:481–488. [PubMed: 17514200]

Gross CG. Neurogenesis in the adult brain: death of a dogma. Nat Rev Neurosci 2000;1:67–73. [PubMed: 11252770]

Ihrie RA, Alvarez-Buylla A. Cells in the astroglial lineage are neural stem cells. Cell Tissue Res 2008;331:179–191. [PubMed: 17786483]

Kriss JP, Maruyama Y, Tung LA, Bond SB, Revesz L. The fate of 5-bromodeoxyuridine, 5-bromodeoxycytidine, and 5-iododeoxycytidine in man. Cancer Res 1963;23:260–268. [PubMed: 14035826]

Lavdas AA, Grigoriou M, Pachnis V, Parnavelas JG. The medial ganglionic eminence gives rise to a population of early neurons in the developing cerebral cortex. J Neurosci 1999;19:7881–7888. [PubMed: 10479690]

Letinic K, Zoncu R, Rakic P. Origin of GABAergic neurons in the human neocortex. Nature 2002;417:645–649. [PubMed: 12050665]

Liu YW, Curtis MA, Gibbons HM, Mee EW, Bergin PS, Teoh HH, Connor B, Dragunow M, Faull RL. Doublecortin expression in the normal and epileptic adult human brain. Eur J Neurosci 2008;28:2254–2265. [PubMed: 19046368]

Luzzati F, Bonfanti L, Fasolo A, Peretto P. DCX and PSA-NCAM expression identifies a population of neurons preferentially distributed in associative areas of different pallial derivatives and vertebrate species. Cereb Cortex 2009;19:1028–1041. [PubMed: 18832334]

Marin-Padilla M. Dual origin of the mammalian neocortex and evolution of the cortical plate. Anat Embryol (Berl) 1978;152:109–126. [PubMed: 637312]

Meyer G, Soria JM, Martinez-Galan JR, Martin-Clemente B, Fairen A. Different origins and developmental histories of transient neurons in the marginal zone of the fetal and neonatal rat cortex. J Comp Neurol 1998;397:493–518. [PubMed: 9699912]

Nacher J, Crespo C, McEwen BS. Doublecortin expression in the adult rat telencephalon. Eur J Neurosci 2001;14:629–644. [PubMed: 11556888]

Ohira K, Furuta T, Hioki H, Nakamura KC, Kuramoto E, Tanaka Y, Funatsu N, Shimizu K, Oishi T, Hayashi M, Miyakawa T, Kaneko T, Nakamura S. Ischemia-induced neurogenesis of neocortical layer 1 progenitor cells. Nat Neurosci 2010;13:173–179. [PubMed: 20037576]

Packard DS Jr, Menzies RA, Skalko RG. Incorportaiton of thymidine and its analogue bromodeoxyuridine, into embryos and maternal tissues of the mouse. Differentiation 1973;1:397–404. [PubMed: 4802502]

Pekcec A, Loscher W, Potschka H. Neurogenesis in the adult rat piriform cortex. Neuroreport 2006;17:571–574. [PubMed: 16603913]

Raedler E, Raedler A. Autoradiographic study of early neurogenesis in rat neocortex. Anat Embryol (Berl) 1978;154:267–284. [PubMed: 707818]

Rakic P. Mode of cell migration to the superficial layers of fetal monkey neocortex. J Comp Neurol 1972;145:61–83. [PubMed: 4624784]

Rakic S, Zecevic N. Emerging complexity of layer I in human cerebral cortex. Cereb Cortex 2003;13:1072–1083. [PubMed: 12967924]

Seki T, Arai Y. Expression of highly polysialylated NCAM in the neocortex and piriform cortex of the developing and the adult rat. Anat Embryol 1991;184:395–401. [PubMed: 1952111]

Shapiro LA, Ng KL, Kinyamu R, Whitaker-Azmitia P, Geisert EE, Blurton-Jones M, Zhou QY, Ribak CE. Origin, migration and fate of newly generated neurons in the adult rodent piriform cortex. Brain Struct Funct 2007;212:133–148. [PubMed: 17764016]

Shapiro LA, Ng K, Zhou QY, Ribak CE. Subventricular zone-derived, newly generated neurons populate several olfactory and limbic forebrain regions. Epilepsy Behav 2009;14:74–80. [PubMed: 18849007]

Sirko S, Neitz A, Mittmann T, Horvat-Bröcker A, von Holst A, Eysel UT, Faissner A. Focal laser-lesions activate an endogenous population of neural stem/progenitor cells in the adult visual cortex. Brain 2009;132:2252–2264. [PubMed: 19286696]

Srikandarajah N, Martinian L, Sisodiya SM, Squier W, Blumcke I, Aronica E, Thom M. Doublecortin expression in focal cortical dysplasia in epilepsy. Epilepsia 2009;50:2619–2628. [PubMed: 19583780]

Tashiro A, Makino H, Gage FH. Experience-specific functional modification of the dentate gyrus through adult neurogenesis: a critical period during an immature stage. J Neurosci 2007;27:3252–3259. [PubMed: 17376985]

Taupin P. BrdU immunohistochemistry for studying adult neurogenesis: paradigms, pitfalls, limitations, and validation. Brain Res Rev 2007;53:198–214. [PubMed: 17020783]

Tonchev AB, Yamashima T, Sawamoto K, Okano H. Enhanced proliferation of progenitor cells in the subventricular zone and limited neuronal production in the striatum and neocortex of adult macaque monkeys after global cerebral ischemia. J Neurosci Res 2005;81:776–788. [PubMed: 16047371]

von Bohlen Und Halbach O. Immunohistological markers for staging neurogenesis in adult hippocampus. Cell Tissue Res 2007;329:409–420. [PubMed: 17541643]

Wichterle H, Turnbull DH, Nery S, Fishell G, Alvarez-Buylla A. In utero fate mapping reveals distinct migratory pathways and fates of neurons born in the mammalian basal forebrain. Development 2001;128:3759–3771. [PubMed: 11585802]

Wojtowicz JM. Irradiation as an experimental tool in studies of adult neurogenesis. Hippocampus 2006;16:261–266. [PubMed: 16435311]

Xiong K, Luo DW, Patrylo PR, Luo XG, Struble RG, Clough RW, Yan XX. Doublecortin-expressing cells are present in layer II across the adult guinea pig cerebral cortex: partial colocalization with mature interneuron markers. Exp Neurol 2008;211:271–282. [PubMed: 18378231]

Zecevic N, Rakic P. Development of layer I neurons in the primate cerebral cortex. J Neurosci 2001;21:5607–5619. [PubMed: 11466432]

Zhang XM, Cai Y, Chu Y, Chen EY, Feng JC, Luo XG, Xiong K, Struble RG, Clough RW, Patrylo PR, Kordower JH, Yan XX. Doublecortin-expressing cells persist in the associative cerebral cortex and amygdala in aged nonhuman primates. Front Neuroanat 2009;3:17. [PubMed: 19862344]

Zhao C, Deng W, Gage FH. Mechanisms and functional implications of adult neurogenesis. Cell 2008;132:645–660. [PubMed: 18295581]

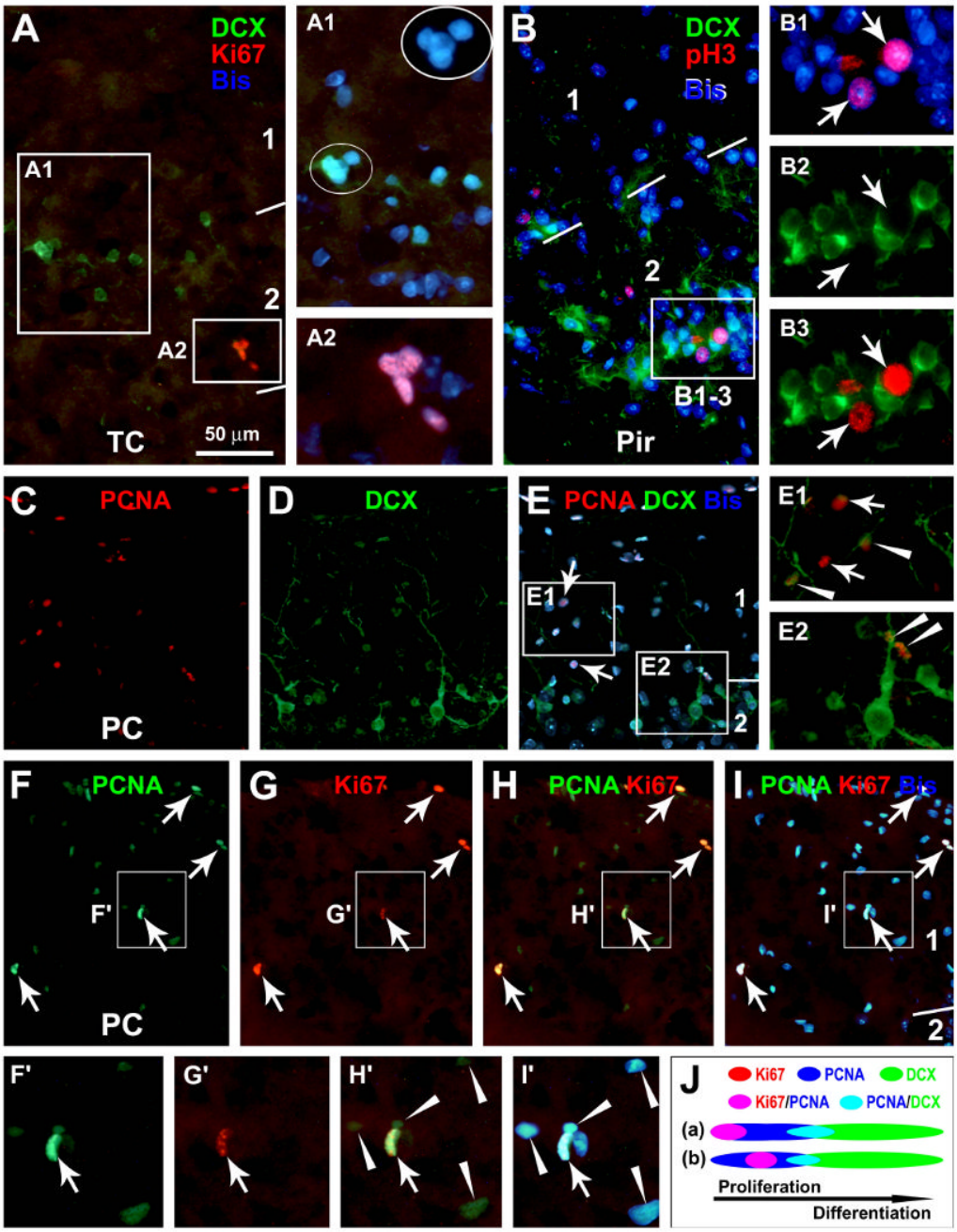

Fig. 1.

Representative images from 3 month-old guinea pigs showing the expression of endogenous proliferative markers, Ki67 (Ki67+), phosphorylated histone-3 (pH3+) and proliferation cell nuclear antigen (PCNA+), around layers I and II in relevance to doublecortin-expressing (DCX+) cells. Ki67+ (A-A2), pH3+ (B-B3) and PCNA+ (C-E2) nuclei occur discretely in layers I and II, including at the pial mater, with some labeled cells appear in pairs (C-I) or small clusters (A). Ki67+ and pH3+ cells may locate next to DCX+ cells in layer II (A, B), whereas PCNA co-localizes in some small DCX+ cells (C-E) (arrowheads). Among the PCNA+ nuclei, Ki67 co-expresses in those with heavy (arrows), but not those with weak (arrowheads), PCNA reactivity (F-I and F′-I′). The schematic draw (J) illustrates hypothetic temporal relationships for Ki67, pH3, PCNA and DCX expressions in layer I/II cells. Ki67/

pH3 expression may begin at the same time (a) or somewhat later (b) but last shorter relative to PCNA during mitotic cell cycle. Arab numbers indicate cortical layers. Bisbenzimide (Bis) nuclear stain is shown in blue. TC: temporal cortex; Pir: piriform cortex; PC: parietal cortex. Scale bar in (A) = 50 μm applying to (B, E1, E2), equivalent to 25 μm for A1, A2, B1-B3, F′-I′; and 100 μm for (C-I).

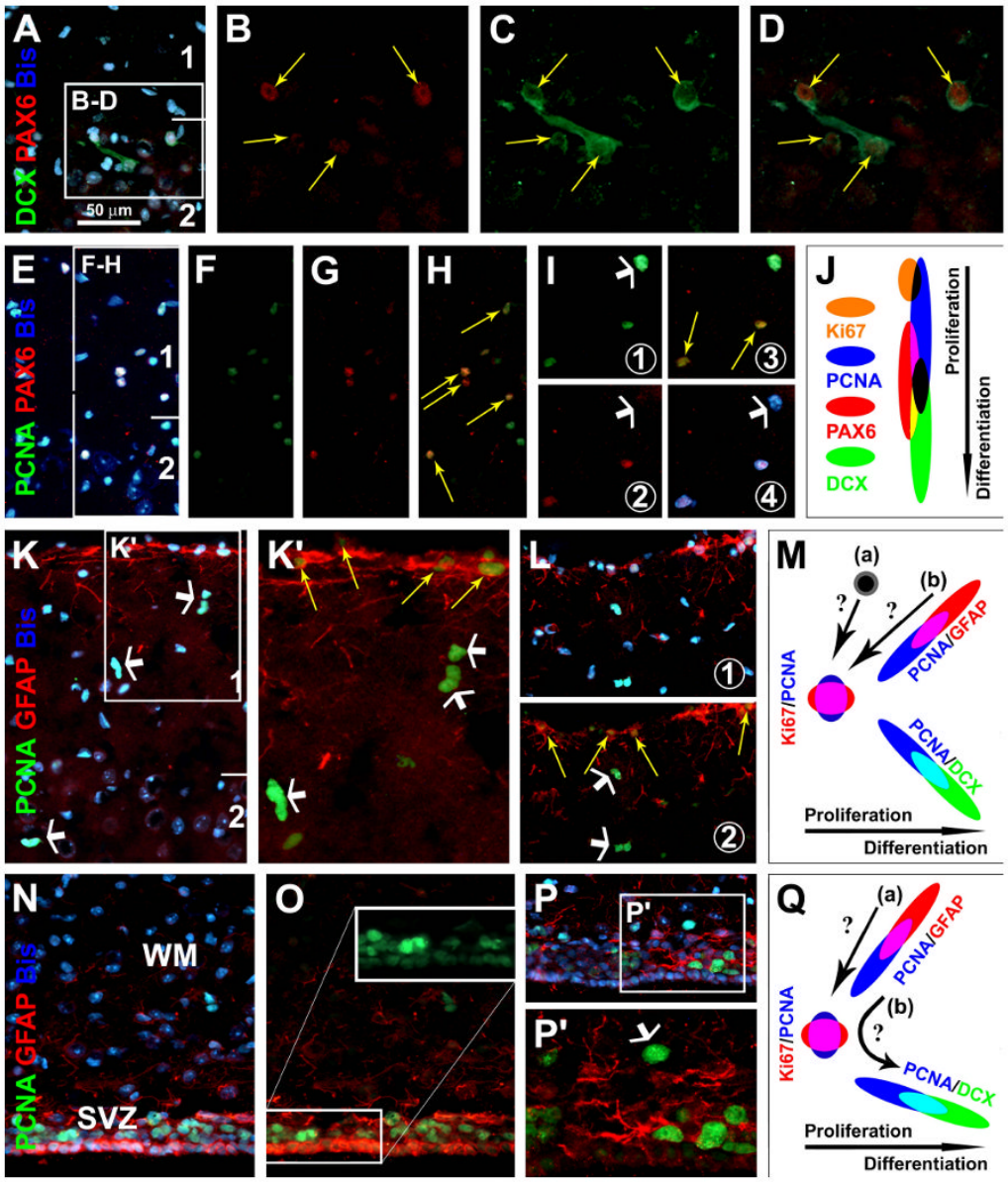

Fig. 2.

Partial colocalization of the Paired Box Protein Pax-6 (PAX6) with DCX (A-D) or PCNA (E-I) around layers I/II, and PCNA with glial fibrillary acidic protein (GFAP) in layers I (K-L) and the periventricular site (N-P) (images were from 6 month-old guinea pigs). PAX6 co-exists in DCX+ cells around layer II (yellow arrows), more distinct in small relative to large cells (A-D). PAX6 is partially colocalized among PCNA+ cells, in those with weak (yellow arrows) but not in those with heavy (white arrows) PCNA reactivity (E-I). GFAP+ cells around the pia may co-express weak PCNA (yellow arrows), whereas subpial PCNA nuclei (white arrows) lack GFAP colocalization (K, L). Around the lateral ventricle, PCNA and GFAP colocalize in ependymal layer cells (N-P). Schematic draw (J) depicts a hypothetic sequence of Ki67, PCNA, PAX and DCX expression among layers I/II cells, based on the partial colocalization patterns among these markers. Panel (M) hypothesizes two scenarios whereby the heavy-reactive PCNA cells around layer I may arise, from either specific proliferative layer I cells (a) or pia-associated GFAP+/PCNA+ cells (b). Panel (Q) depicts a

potential astrocytic origin of immature neurons (PCNA+ → DCX+) around the subventricular zone (SVZ) (Ihrie and Alvarez-Buylla, 2008), either directly evolving from GFAP+/PCNA+ cells (b) or via a proliferative intermediate form (a). WM: white matter. Scale bar in (A) = 50 μm applying to (E-I, K, L-P), equivalent to 25 μm for B-D, K′ and P′.

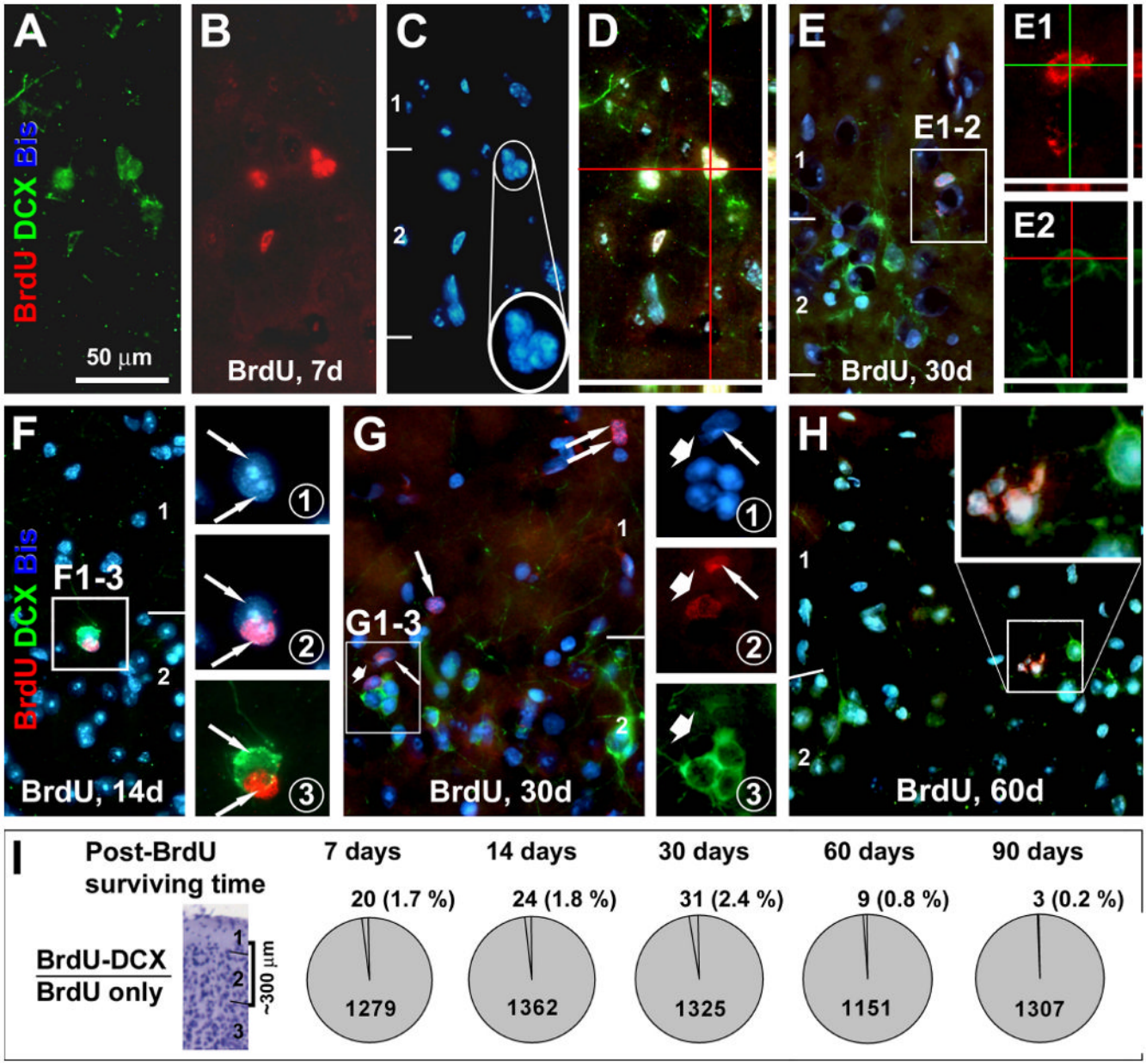

Fig. 3.

Low rate 5-bromodeoxyuridine (BrdU) colocalization in DCX+ cells around layer II at various time points after BrdU administration. Panels (A-D) and (E-E2) show examples of BrdU-incorporated DCX+ cells at the layers I/II border (from animals surviving 7 and 30 days). BrdU reactivity occurs in the nucleus counterstained with bisbenzimide (Bis, blue) across the thickness (6 μm) of the section as verified by confocal Z-score scanning (D, E1, E2). Note that BrdU+/DCX+ cells may appear in clusters (C), and that the double-labeled cells have no or barely-visible dendritic processes (A, E2). Single-labeled BrdU+ cells may occur next to single-labeled DCX+ cells, with their cell bodies tightly apposing to each other seemingly forming the same cluster (F-F3 and G-G3). Also note that BrdU+ cells may occur in pairs or cluster around layers I and II (G), with some appeared to be shrinking or deformed (H). Pie-graphs (I) summarize the percentages of BrdU+/DCX+ relative to total BrdU+ cells at 7-90 surviving days post-BrdU application, based on cell counts over ~300

μm depth around the junction of layers I and II. Scale bar in (A) = 50 μm applying to main panels (B-H), equivalent to 25 μm in (E1, E2; F1-3 and G1-3) and 12.5 μm in enlarged inserts in (C and H).

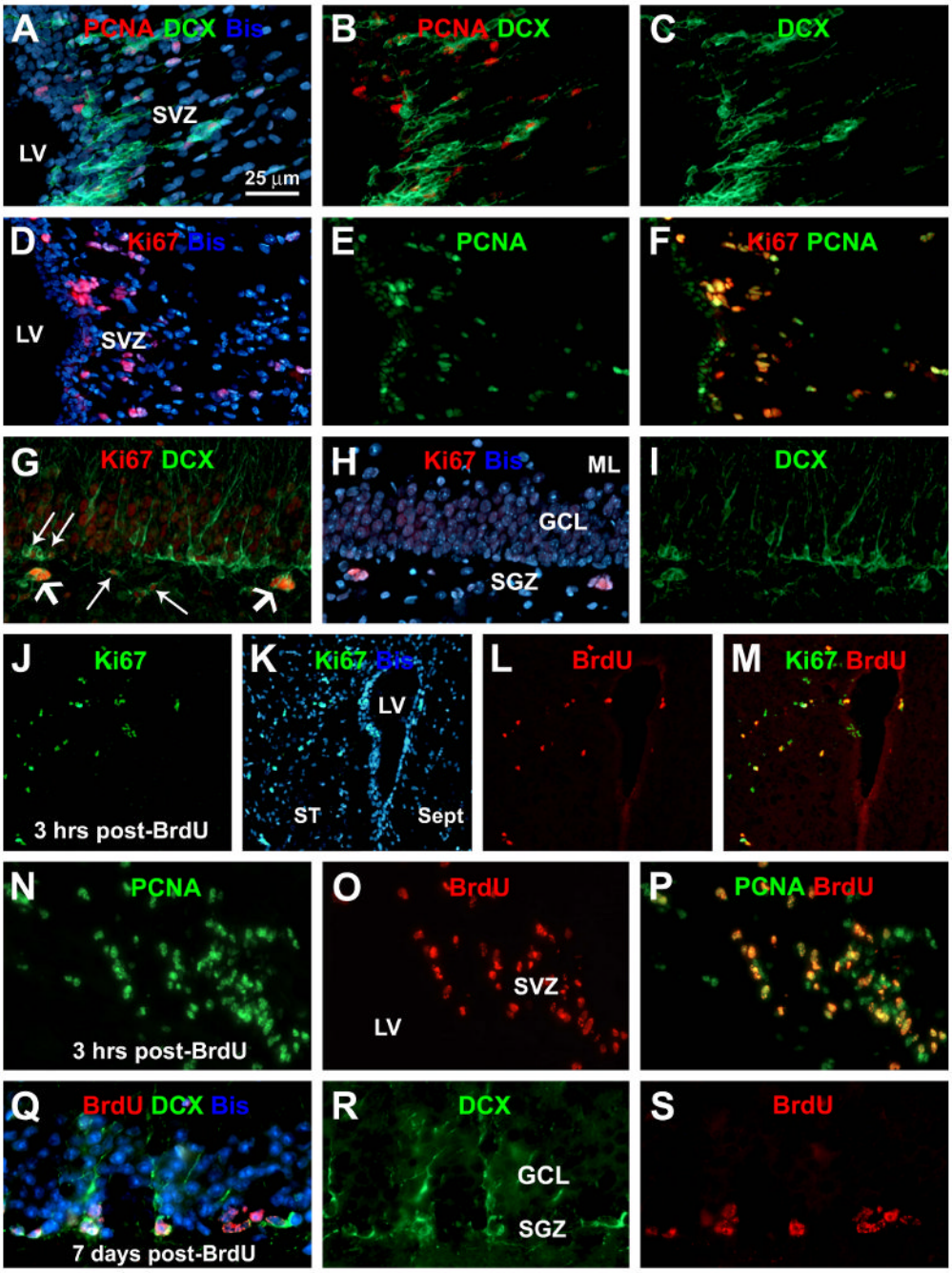

Fig. 4.

Cross-validation for the expression of proliferation index markers in relevance to neurogenesis around the subventricular and subgranular zones (SVZ, SGZ). Panels (A-C) show partial colocalization of PCNA in DCX+ cells at the SVZ. Panels (D-F) show Ki67 expression in heavy but not light reactive PCNA+ nuclei in the SVZ. Panels (G-I) show Ki67 expression in DCX+ cell clusters at the SGZ. Panels (J-P) show partial colocalization of BrdU in Ki67+ (J-M) and PCNA+ (N-P) cells around the SVZ at 3 hours after a single BrdU injection. At 7 days post-BrdU administration, BrdU labeling is found in DCX+ cells at the SGZ that have well-formed dendrites extending into the molecular layer (Q-S). Scale bar in (A) = 25 μm applying to (B-I, N-S), equivalent to 100 μm for (J-M).

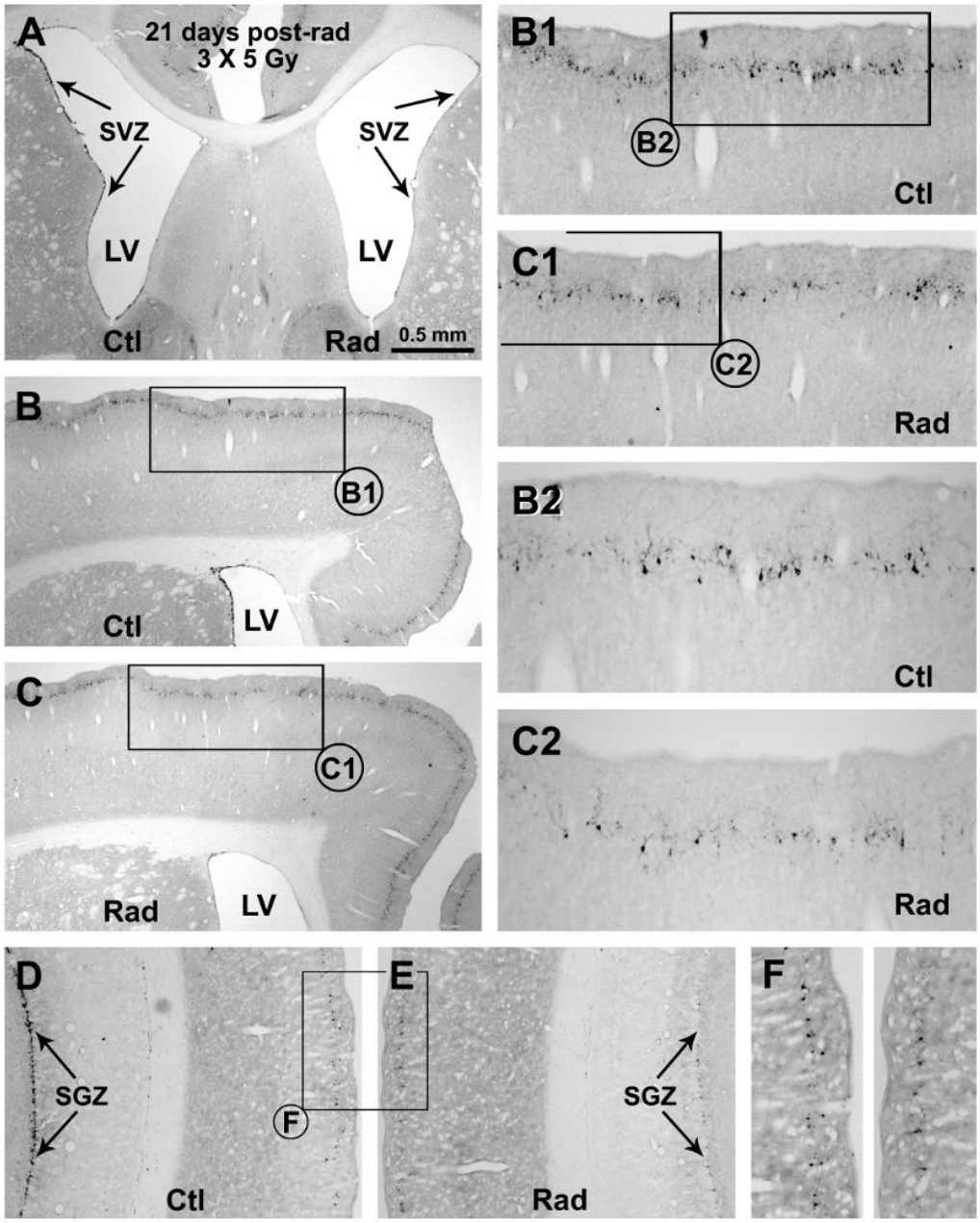

Fig. 5.

Representative images showing decline of DCX+ cells in the subventricular ventricular zone (A-C), subgranular granular zone (D, E) and around layer II of the neocortex (B-F) in the radiated (Rad) relative to the control (Ctl) sides 21 days after unilateral cranial X-ray irradiations (on day 1, 7 and 14). Framed areas in (B, C, D, E) are enlarged sequentially as indicated (B1, B2, C1, C2, F). Scale bar in (A) = 500 μm applying to (D, E), equivalent to 250 μm for (B1, C, F) and 125 μm for (B2, C2).

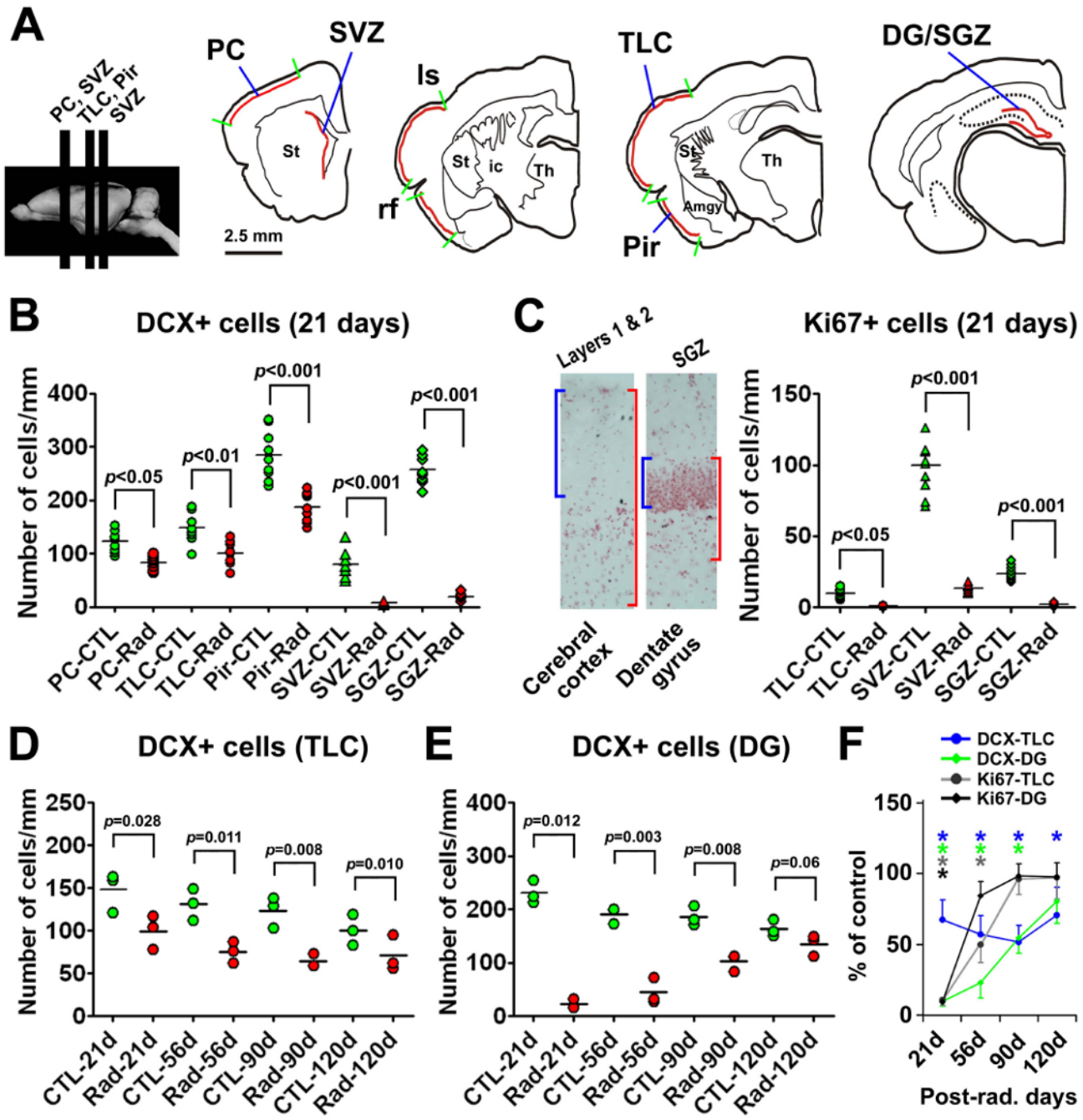

Fig. 6.

Quantitative data summarizing post-radiation declines of DCX+ and Ki67+ cells in representative forebrain areas. Drawings in (A) show the rostrocaudal levels of sections used for cell counts, including the parietal cortex (PC) and subventricular zone (SVZ) passing the striatum, the temporal lobe cortex (TLC) between the lateral sulcus (ls) and the rhinal fissure (rf) and the piriform cortex (Pir) inferior to the rhinal fissure passing the amygdala, and the dentate gyrus (DG) or SGZ passing the mid-hippocampus. For counting Ki67+ cells in the cortex, the area of interest consists of a tangential cortical band, with its perpendicular distance extending from the pia down to two times of the depth of layer I (C). For counting Ki67+ cells in the DG, the area of interest is defined as to include the granular cell layer

(GCL) and a subgranular band with its depth equivalent to that of the GCL. Relative densities of DCX+ and Ki67 cells are calculated as the number of cells in the measured areas divided by the corresponding lengths of the pial surface, the ventricular wall or the GCL. Dot-graph (B) shows DCX+ cell densities in the radiated (Rad) and control (CTL) sides in individual sections (3 levels/region/brain) 21 days post-radiation. Panel (C) shows significant reductions of Ki67+ cells in the TLC as well as the SVZ/SGZ at 21 days post-radiation. Dot graphs (D) and (E) show DCX+ cell densities (means of individual brains) in the radiated and control TLC (D) and DG (E), respectively at 21, 56, 90 and 120 days post-radiation. Line-graph (F) shows the relative levels (%) of DCX+ and Ki67+ cells in the radiated TLC and DG normalized to corresponding controls (defined as 100%) at the above post-radiation time points. *P* values (B-E) and asterisks (F) indicate statistically significant difference between comparing means (one-way ANOVA for B, C; and one-tailed Students-*t* test for D-F).

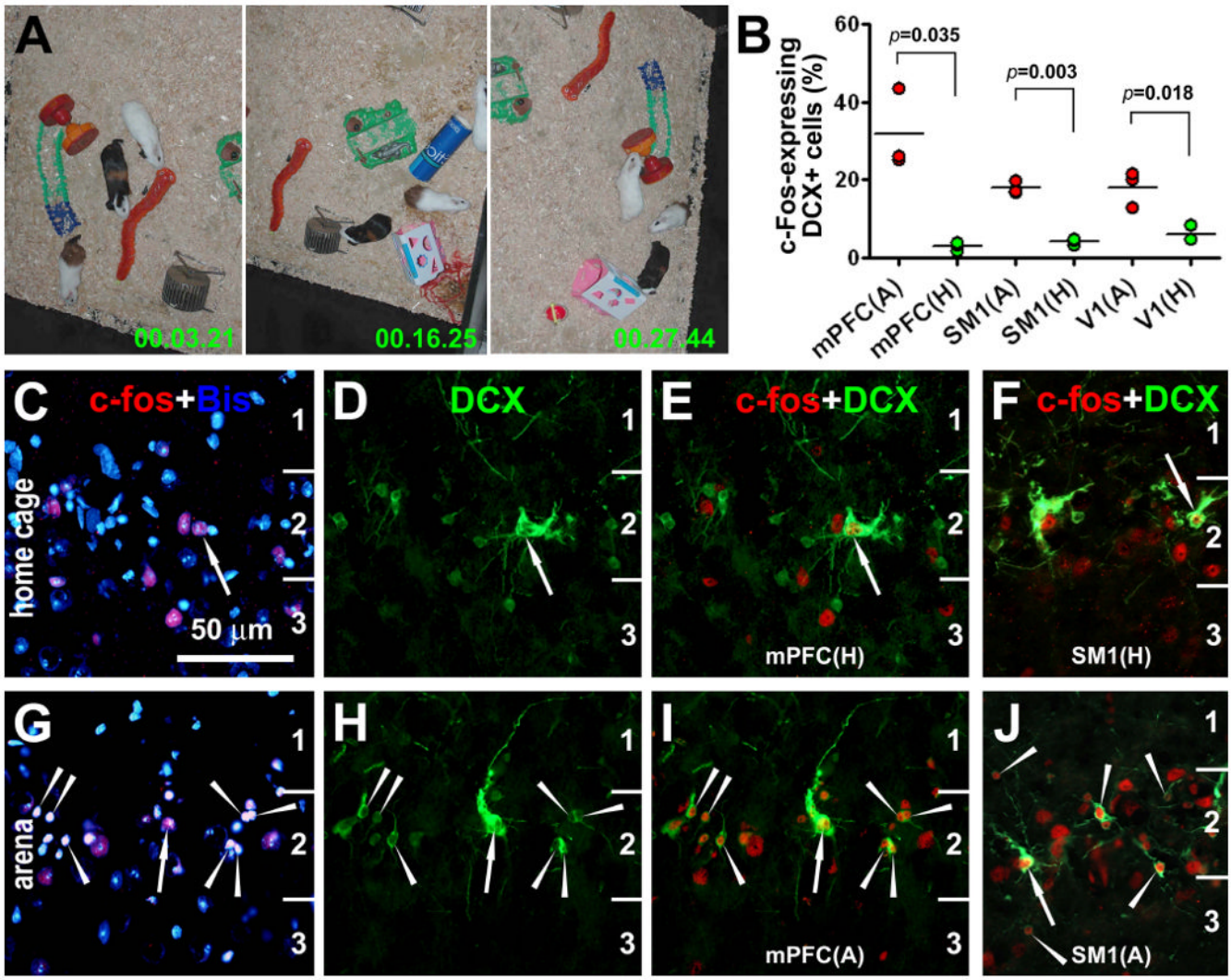

Fig. 7.

c-Fos induction in cortical DCX+ cells in young guinea pigs following novel environmental exploration. Video digital images (A) indicate explorative behavior of the animals during the 30 minute period of exposure to a novel arena. Dot-graph (B) shows an increased rate (%) of c-Fos-expressing DCX+ cells counted in the medial prefrontal (mPFC), primary somatosensory (SM1) and primary visual (V1) cortices in the experimental (A-arena) animals (n=3) relative to home-caged controls (H-home) (n=3) as assessed by students-*t* tests. Double fluorescent images show examples of c-Fos expression in DCX+ cells around layer II from a home-caged control (C-F) and an experimental animal (G-J). Arrows in (C-J) point to large DCX+ cells with well-developed dendritic and axonal processes, whereas arrowheads indicate small DCX+ cells. Scale bar = 50 μm for all fluorescent images.